

Many-body spectral transitions through the lens of variable-range SYK₂ model

Andrea Legramandi,^{1,2,*} Soumik Bandyopadhyay,^{1,2,†} and Philipp Hauke^{1,2,‡}

¹*Pitaeuskii BEC Center, CNR-INO and Dipartimento di Fisica, Università di Trento, I38123 Trento, Italy*

²*INFN-TIFPA, Trento Institute for Fundamental Physics and Applications, Trento, Italy*

The Sachdev–Ye–Kitaev (SYK) model is a cornerstone in the study of quantum chaos and holographic quantum matter. Real-world implementations, however, deviate from the idealized all-to-all connectivity, raising questions about the robustness of its chaotic properties. In this work, we investigate a quadratic SYK model with distance-dependent interactions governed by a power-law decay. By analytically and numerically studying the spectral form factor (SFF), we uncover how the single particle transitions manifest in the many-body system. While the SFF demonstrates robustness under slightly reduced interaction ranges, further suppression leads to a breakdown of perturbation theory and new spectral regimes, marked by a higher dip and the emergence of a secondary plateau. Our results highlight the interplay between single-particle criticality and many-body dynamics, offering new insights into the quantum chaos-to-localization transition and its reflection in spectral statistics.

Introduction.—The Sachdev–Ye–Kitaev (SYK) model [1, 2] has emerged as a paradigmatic example in the study of quantum chaos and holographic quantum matter [3–6], thanks to its analytical tractability in the thermodynamic limit [7]. Additionally, it has inspired various proposals for experimental implementation [8–17], which could open the door to studying the theoretically challenging regime of intermediate system sizes, where quantum corrections to gravity become prominent. However, any realistic laboratory implementation would deviate from the idealized SYK model, which assumes all-to-all connectivity and perfectly uncorrelated random couplings. These deviations raise important questions about the robustness of the model’s properties when the interactions are constrained to finite range. The introduction of distance-dependent interactions, as is typical for platforms such as trapped ions [18–21], cold atoms and molecules [22–24], solid state systems [25], etc., is expected to considerably impact the system’s chaotic behavior [26] and can potentially lead to significant many-body phenomena such as non-ergodicity and localization [27–39], which are central to understanding the quantum dynamics of strongly coupled but not chaotic systems.

In this work, we aim at unveiling the transitions of a system composed of N Majorana fermions with random hopping suppressed by a power-law decay $r^{-\alpha}$ (see Fig. 1a)—a version of the quadratic SYK whose underlying single-particle physics described by a power-law random banded model (PRBM) [40]. The PRBM has become a popular model for studying Anderson criticality [41] and multifractality [42, 43], as it is amenable to analytical studies using the supersymmetric sigma-model approach [44]. Here, we take a different route: we study the many-body spectral statistics of the SYK model using the spectral form factor (SFF) [45]. In the thermodynamic limit, it can be treated analytically thanks to a path integration [46], which results in a different sigma model than the supersymmetric one.

The SFF, introduced in the context of random ma-

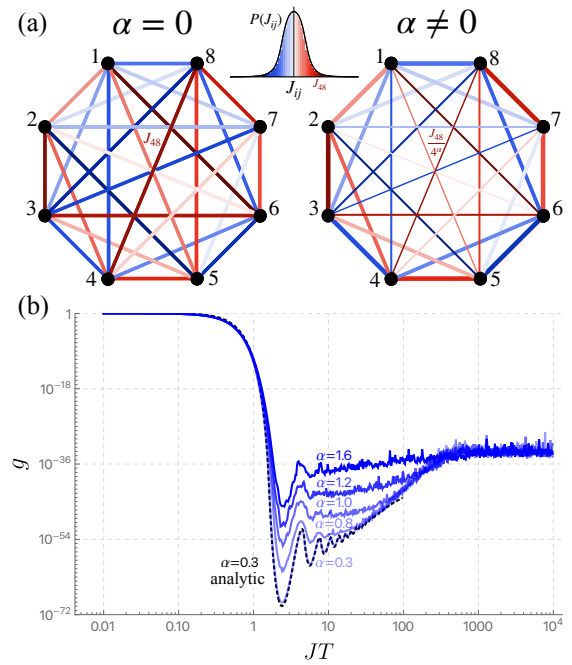


FIG. 1: (a) Illustration of the model in Eq. (1) for $N = 8$ Majorana fermions on a circle, with all-to-all random couplings drawn from a Gaussian distribution. The line thickness represents the interaction strength, which decays with distance as $r^{-\alpha}$. (b) The SFF g for $N = 20$ fermions, for increasing α from light to dark blue shades. For $\alpha < 1/2$, the numerical results align well with the analytical prediction from Eq. (15) (black dashed line). For $\alpha > 1/2$, the system moves beyond the validity regime of the analytical approach, leading to a higher dip and the emergence of a secondary plateau, which merges with the late-time plateau for $\alpha \gtrsim 3/2$.

trix theory [45], reflects the distribution of energy levels in a system. In chaotic systems, the SFF typically exhibits a universal structure characterized by an initial

non-universal slope, a dip, a linear ramp, and a late-time plateau. However, in non-chaotic systems, the SFF loses this universal behavior and is less well understood [47–62]. For example, in the quadratic SYK model, the SFF displays an exponential ramp instead of a linear one [63, 64], highlighting that the system is chaotic only at the single-particle level.

Our model allows us to take this analysis further by investigating how the transitions that are present in the single-particle PRBM affect the many-body system, and in particular to determine how the SFF can serve as a marker for them. As the interaction range starts to decrease, a saddle point calculation reveals that the SFF is only subleadingly affected, demonstrating that the theory is robust and preserves ergodicity. However, if we further decrease the interaction range (beyond $\alpha \sim 0.5$), perturbation theory breaks down and a transition occurs marked by distinctive changes in the SFF (Fig. 1b): a growth of the dip and the emergence of a secondary plateau, indicative of a pre-thermalization regime [48, 58] where the Hilbert space is not fully explored [59]. These features allow us to identify how single-particle transitions get imprinted onto transitions in the many-body level statistics and to interpret their physical significance.

Model.—The variable-range SYK₂ model is a variant of the SYK₂ Hamiltonian where the random two-fermion term is weighted by a function of the distance between the two sites involved,

$$\mathcal{H} = \frac{i}{\mathcal{N}} \sum_{i < j}^N J_{ij} a(i-j) \psi_i \psi_j, \quad (1)$$

$$a(i-j) = (\min\{|i-j|, N-|i-j|\})^{-\alpha}.$$

The couplings J_{ij} are real Gaussian variables with variance $\langle J_{ij} J_{kl} \rangle = \mathcal{J}^2 \delta_{ik} \delta_{jl}$ and the Majorana fermions are distributed on a line with periodic boundary conditions. For later convenience, we also define the circular matrix A with entries

$$A_{ij} = [a(i-j)]^2 / \mathcal{N}^2, \quad A_{ii} = 0, \quad (2)$$

with $\mathcal{N}^2 = \sum_i [a(i)]^2$ chosen such that the Hamiltonian is extensive.

The one-particle Hamiltonian $J_{ij} a(i-j)$ is an example of a PRBM. These models exhibit different properties depending on the value of α [40]: for $\alpha \in [0, 0.5)$, the system is ergodic and indistinguishable from the Gaussian orthogonal ensemble. For $\alpha > 1.5$, it becomes integrable [65]. At $\alpha = 1$, it has an Anderson critical point [40, 41, 66–69] separating the delocalized but non-ergodic regime $\alpha \in (0.5, 1)$ [65, 70, 71], from the localized but super-diffusive regime $\alpha \in (1, 1.5)$. The remainder of this paper explores how these one-particle transitions manifest in the many-body system.

Path integral for the SFF.—The main quantity we will use to analyze the many-body physics is the SFF,

defined as $g(T) = \langle |Z(iT)|^2 \rangle / \langle |Z(0)|^2 \rangle$. The angle brackets denote averaging over the random couplings. In what follows, we will express $g(t)$ in terms of collective-field variables, find the dominant saddle point solutions, which spontaneously break some of the symmetries of the action, and identify the contribution from the associated zero modes, which depend on the eigenvalues of the matrix A defined in Eq. (2).

First, we express the partition function as a path integral,

$$Z(iT) = \int \mathcal{D}\psi \exp \left\{ \int_0^T \left(-\sum_i \frac{1}{2} \psi_i \partial_t \psi_i + i\mathcal{H} \right) dt \right\}, \quad (3)$$

leading to

$$g(T) = \int \mathcal{D}\psi^L \mathcal{D}\psi^R \left\langle \exp \left\{ i \int_0^T dt (\mathcal{H}[\psi^R] - \mathcal{H}[\psi^L]) \right\} \right\rangle$$

$$\times \exp \left\{ -\frac{1}{2} \sum_i \int_0^T dt (\psi_i^L \partial_t \psi_i^L + \psi_i^R \partial_t \psi_i^R) \right\}, \quad (4)$$

where the denominator has been absorbed in the measure and ψ_i^L are the Grassmannian variables of $Z(-iT)$ while ψ_i^R the ones of $Z(iT)$.

After the Gaussian integration over the couplings, we can introduce collective fields in order to make the action quadratic in the fermions. In the usual SYK case, these are given by an averaged two-point function $G^{ab}(t, t') = \frac{1}{\mathcal{N}} \sum_i \psi_i^a(t) \psi_i^b(t')$, with $a, b = L, R$. In contrast, to account for the spatial profile of the power-law coupling, we introduce a local two-point function $G_i^{ab}(t, t') = \psi_i^a(t) \psi_i^b(t')$, similarly to [72]. Imposing this definition at the path-integral level requires the introduction of an auxiliary field $\Sigma_i^{ab}(t, t')$. Afterwards, we can perform two Gaussian integrals, one over the fermions and the other one over G_i^{ab} . These manipulations, which are detailed in [73], lead to

$$g(T) = \int \mathcal{D}\Sigma_i e^{-I[\Sigma_i]}, \quad (5)$$

$$I = -\frac{1}{2} \sum_i \text{Tr} \log(\partial - i\Sigma_i) + \sum_{abij} \frac{(-)^{a+b}}{4\mathcal{J}^2} \iint_0^T A_{ij}^{-1} \Sigma_i^{ab} \Sigma_j^{ab},$$

where the trace is over times and the L, R indices, and where we have defined $\partial_{at, bt'} = \delta(t-t') \delta_{ab} \partial_{t'}$.

Saddle point equation.—Varying the effective action in Eq. (5) with respect to Σ and assuming time-translation invariance, we get the saddle-point equation in frequency space

$$\frac{1}{\mathcal{J}^2} \sum_j A_{ij}^{-1} \Sigma_j^{ba}(-\omega_n) = -(-)^{a+b} (\omega_n \delta^{ab} - \Sigma_i^{ab}(\omega_n))^{-1}, \quad (6)$$

where $\omega_n = (2n+1)\pi/T$ are Matsubara frequencies with $n \in \mathbb{Z}$. As discussed in [73], this equation has a $SU(2)$

symmetry for each (positive) Matsubara frequency given by the adjoint action on the matrix indices of Σ , defining an infinite-dimensional symmetry group.

In principle, this equation may allow for several possible solutions. However, we will work in the ansatz where the dominating saddle does not depend on the site position. This assumption is consistent since averaging over the couplings restores space translation symmetry, and the numerics suggest the slope part of the SFF, which is determined by the classical action, does not depend on α as long as the single-particle PRBM is ergodic, i.e., as long as $\alpha < 1/2$ [74]. We do expect deviations from this behaviour for larger α , when the PRBM localizes and non-uniform saddle-point solutions can emerge. By imposing $\Sigma_i^{ab} = \tilde{\Sigma}^{ab}$, it is possible to obtain the same dominant saddles as in the $\alpha = 0$ case [73]:

$$\tilde{\Sigma}^{ab}(\omega_n) = \begin{cases} \frac{1}{2}(\omega_n - \sqrt{\omega_n^2 - 4J^2})\delta_{ab} & \omega_n > 2J, \\ \frac{1}{2}(\omega_n\delta_{ab} - i\sqrt{4J^2 - \omega_n^2}\sigma_3^{ab}) & 0 < \omega_n < 2J. \end{cases} \quad (7)$$

The solutions for negative frequencies can be recovered using $\tilde{\Sigma}^{ab}(-\omega_n) = -\tilde{\Sigma}^{ba}(\omega_n)$. One can check that the effective action evaluated on the homogeneous saddle point becomes linear in N , increasing the reliability of the semiclassical approximation with N as in the usual SYK model.

Notably, for $|\omega_n| > 2J$, $\tilde{\Sigma}$ is proportional to the identity and therefore invariant with respect to the adjoint action of the SU(2) symmetry discussed in [73], while this

is not the case for $|\omega_n| < 2J$. In the latter regime, the classical solution spontaneously breaks SU(2) to U(1). The transformation in the coset space SU(2)/U(1) generates new equivalent solutions, leading to a contribution to the path integral proportional to the coset volume. This symmetry-breaking pattern resembles the one in SYK₄, where the ramp is generated by a spontaneous symmetry breaking of the U(1) time translation symmetry. Since our model is a free theory, we have a larger symmetry group that gets spontaneously broken.

Quadratic fluctuations.—The above symmetry-breaking pattern suggests the presence of zero modes, which are responsible for the leading correction to the classical action and the development of the ramp in the SFF. As pointed out in Ref. [63], the ramp originates from the fact that, as T increases, more Matsubara modes enter the symmetry breaking regime $|\omega_n| < 2J$, each bringing a contribution proportional to the coset volume. Differently from Ref. [63], however, the long-range decay can influence the number of the zero modes.

To rigorously identify them, we analyse the Gaussian fluctuations around the saddle point solution

$$\Sigma_i^{ab}(t, t') = \tilde{\Sigma}^{ab}(t, t') + \delta\Sigma_i^{ab}(t, t'). \quad (8)$$

To expand the effective action up to the second order in $\delta\Sigma$, it is convenient to write $\delta\Sigma$ in frequency space and to use a basis that diagonalizes A . Denoting its eigenvalues as λ_k , we have

$$g(T) = e^{-I_{\text{cl}}} \int \mathcal{D}\delta\Sigma_i \exp \left\{ \frac{1}{4J^2 T^2} \sum_{k,a,b,\omega_1,\omega_2} \delta\Sigma_k^{ab}(\omega_1, \omega_2) K_k^{ab}(\omega_1, \omega_2) \Sigma_k^{ba}(-\omega_2, -\omega_1) \right\}, \quad (9)$$

where I_{cl} is the classical action contribution and

$$K_k^{ab}(\omega_1, \omega_2) = \frac{(-)^{a+b}}{\lambda_k} - \frac{1}{J^2} \tilde{\Sigma}^{aa}(\omega_1) \tilde{\Sigma}^{bb}(-\omega_2). \quad (10)$$

The zero modes correspond to $K_k^{ab}(\omega_1, \omega_2) = 0$, which can only occur in the symmetry-breaking saddle $|\omega_{1,2}| < 2J$ for $a \neq b$ and $\omega_1 = \omega_2$. For this case, Eq. (10) reduces to

$$K_k^{ab}(\omega, \omega) = -\lambda_k^{-1} + 1. \quad (11)$$

Therefore, the exponential ramp is generated by modes with eigenvalues $\lambda_k = 1$.

Eigenvalues of A .—Since A is a circulant matrix, it can be easily diagonalized by going into Fourier space [73]. In particular, the constant vector is an eigenvector with eigenvalue $\lambda_{k=0} = 1$, so we always have at least one

zero mode. In general the eigenvalues are [75]

$$\lambda_k = \frac{\sum_{\Delta=1}^{N/2} \Delta^{-2\alpha} \cos\left(\frac{2\pi}{N} \Delta k\right)}{\sum_{\Delta=1}^{N/2} \Delta^{-2\alpha}}. \quad (12)$$

The limit $N \rightarrow \infty$ must be taken with care since both numerator and denominator can diverge. Analytic formulas can be derived easily for large N and large, respectively, small k [73]. The eigenvalues corresponding to modes with $k \propto N$ are given by

$$\lambda(\tilde{k}) = \begin{cases} 0 & \alpha \leq 1/2, \\ \frac{\text{Re}(\text{Li}_{2\alpha}(e^{i\tilde{k}}))}{\zeta(2\alpha)} & \alpha > 1/2, \end{cases} \quad (13)$$

where Li is the polylogarithm and where we defined $\tilde{k} = \frac{2\pi}{N} k$, $-\pi < \tilde{k} < \pi$. The eigenvalues of the modes with

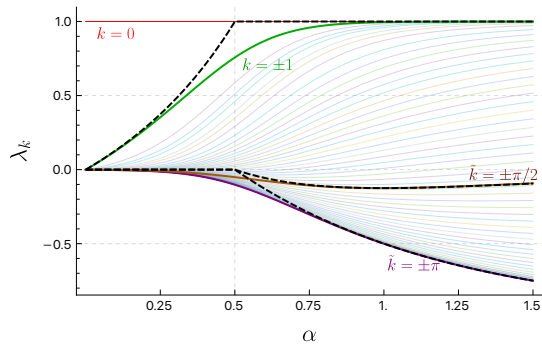


FIG. 2: Eigenvalues λ_k computed numerically for $N = 1001$ (colored) and analytically at $N \rightarrow \infty$ (black dashed). A transition is signaled by the non-differentiable point at $\alpha = 1/2$.

$k = O(1)$, instead, are

$$\lambda_k = \begin{cases} (-1)^k + \frac{\pi^2 k^2}{3-2\alpha} {}_1F_2\left(\frac{3-2\alpha}{2}; \frac{3}{2}, \frac{5-2\alpha}{2}; -\frac{k^2 \pi^2}{4}\right) & \alpha \leq 1/2 \\ 1 & \alpha > 1/2, \end{cases} \quad (14)$$

where ${}_pF_q$ is the generalized hypergeometric function. A comparison between the analytic eigenvalues in the ther-

modynamic limit and the ones computed numerically at finite N can be found in Fig. 2.

A drastic change happens at $\alpha = 1/2$: In Eq. (11), we saw that we have a zero mode whenever $\lambda_k = 1$. The above solutions imply that for $\alpha > 1/2$ an infinite number of zero modes should appear in the thermodynamic limit, each of them bringing a factor proportional to the coset volume. This should lead to a rapid increase of the ramp, i.e., if the saddle point we found is still dominating. However, as we argue in [73], the same behaviour of the eigenvalues breaks down perturbation theory around the uniform saddle (7), signaling that we are entering a new regime where either the physics is described by another saddle or it becomes non-perturbative. Both imply a drastic transition at $\alpha = 1/2$, as in the single-body PRBM.

Analytic SFF.—We have now all the ingredients to present the analytic expression for the SFF (see [73] for details). This is given by the sum of three contributions: the classical action, which is responsible for the slope, the time-symmetric fluctuations, which contain the zero modes and are responsible for the exponential ramp, and the massive fluctuations that are not time symmetric, which are responsible for the late-time corrections to the ramp.

For JT large and for $\alpha < 1/2$, the SFF simplifies to

$$\log \frac{g(T)}{2^N} = N \sum_{j=1}^{\infty} \left[\frac{(-1)^{j+1}}{j} \frac{2J_1(2JjT)}{2JjT} \right] + \frac{JT}{\pi} \log \left(\frac{16}{e^2} \frac{N}{JT} \right) + \frac{JT}{\pi} \sum_{k \neq 0} \left[(1 + \lambda_k) \frac{\operatorname{arctanh} \sqrt{\lambda_k}}{\sqrt{\lambda_k}} - 1 + \log(1 - \lambda_k) \right], \quad (15)$$

where J_1 is a Bessel function of the first kind. Notably, for $\alpha \sim 0$ we have $\lambda_{k \neq 0} \sim N^{-1}$, which means that the λ_k -dependent part is $O(1)$ and hence subleading, so we recover the result in [63]. A comparison between Eq. (15) and numerical data for $\alpha = 0.3$ is presented in Fig. 1b, demonstrating excellent agreement. The $\alpha = 0$ case would be indistinguishable from $\alpha = 0.3$. In general, for $\alpha < 1/2$, the eigenvalue contribution to (15) is subleading, as most eigenvalues vanish in the thermodynamic limit (13). The essentially unmodified form of the SFF highlights that, in the regime $0 \leq \alpha < 1/2$, the variable-range SYK₂ model remains largely unaffected, in agreement with the ergodic phase for PRBM.

SFF and localization.—In this section, we discuss the various regimes of the SFF for $\alpha \geq 1/2$. The PRBM is known to display an ergodic to non-ergodic transition at $\alpha = 1/2$, which is signaled in our analysis by the breakdown of perturbation theory around the uniform saddle point. For $\alpha > 1/2$, PRBM suggests that the system becomes gradually less delocalized, until it enters an integrable regime at $\alpha > 3/2$, while the Anderson critical point is at $\alpha = 1$ [40]. From a path integral point of

view, it is reasonable to expect that, as the system localizes it will break the space translation symmetry we assumed for the saddle-point solution in the small- α region. This is supported by the fact that at early times the SFF takes larger values (in particular at the dip time) than what is predicted analytically, indicating that there may be another saddle that dominates the classical action. This makes the dip height a good candidate for identifying the ergodic/non-ergodic transition. As it can be seen in Fig. 3a, the dip starts to rise considerably in the vicinity of $\alpha \approx 0.5$. A characteristic value of α where there is a qualitative change can be obtained similar to the knee voltage in transistors. In this spirit, the intersection of a linear fit of the large- α part of the curve with the ordinate yields $\alpha = 0.49$.

The regime $1/2 \leq \alpha \leq 3/2$ is characterized by the development of a secondary plateau, as it can be seen in Fig. 1b, which we interpret as a pre-thermalization regime [59]. The height of this secondary plateau grows with α until it reaches the height of the late-time one around $\alpha \sim 3/2$, as expected for an integrable theory. To better quantify this transition, we can consider the

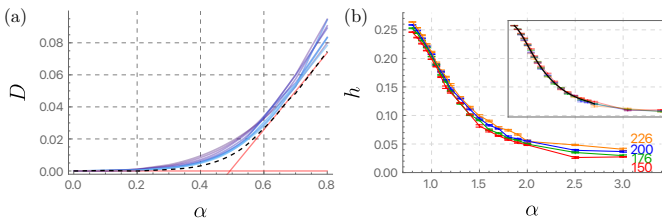


FIG. 3: (a) Dip position as a function of α for different system sizes from $N = 50$ (violet) to 400 (light blue) in steps of 50, averaged over 1M samples. The dip time is given by $T_{\text{Dip}} \sim 2.408$, and we define $D = \frac{1}{N} \log \frac{g(T_{\text{Dip}}, \alpha)}{g(T_{\text{Dip}}, \alpha=0)}$, effectively measuring the shift of the dip relative to the $\alpha = 0$ SFF. The black dashed line shows an extrapolation to $N \rightarrow \infty$. A linear fit to the curve at $\alpha \geq 0.6$ intersects $D = 0$ at a characteristic value of $\alpha = 0.49$. (b) Plateaus distance h , defined in Eq. (16), averaged over $\sim 4 \times 10^7$ samples and at different N . In the inset, the curves are shifted to reveal a universal behavior. The black line represents a fourth-order polynomial fit.

logarithm of the ratio between the two plateau heights,

$$h = \left\langle \frac{1}{N} \log \frac{2^{-N/2}}{g(T)} \right\rangle_T. \quad (16)$$

Here, $2^{-N/2}$ is the theoretical value of the late-time plateau, while the time average is over the interval of time of the first plateau before it starts developing a notable curvature that will bring it into the ramp (we use the interval $JT \in [10, 15]$). The value of h at different N is displayed in Fig. 3b.

By applying a constant shift to h , the curves display an excellent collapse onto each other, as seen in Fig. 3b. A polynomial fourth-order fit of the collapsed curve above $\alpha = 0.8$ reveals a change in concavity at $\alpha = 1.02$, consistent with the PRBM expectation for the Anderson transition. This suggests that the Anderson transition can be identifiable in the SFF as the point where the plateau height grows more quickly.

Within the regime accessible to our numerics it is not possible to see a sharp transition at $\alpha = 3/2$, corresponding in the PRBM to the onset of the integrable regime. We do, however, observe a qualitative disappearance of the ramp (Fig. 1b). To understand whether this PRBM transition is imprinted onto the SFF of our model, it would be desirable to access larger systems sizes, where the secondary plateau is more prominent. However, the SFF for SYK₂ has fluctuations that grow with N^T [76], making it prohibitively expensive to gather sufficient statistics for convergence, which in our case reaches the order of 10^7 samples at $N = 226$. The implications of these large fluctuations are discussed in [73].

Conclusions.—In this paper, we have discussed how the SFF captures the distinct regimes of single-particle

physics in the variable-range SYK₂ model (1). Key features include the dip height, which serves as an indicator of transitions between ergodic and non-ergodic behavior, and the secondary plateau, which arises in the non-ergodic regime and approaches the late-time plateau value as the system becomes localized. The point where the plateau height grows more quickly corresponds to Anderson criticality.

It will be interesting to study these markers in the context of many-body localization. For instance, the dip height has been used as a marker of transitions between holographic and non-holographic behavior in sparse SYK models [60]. Similarly, the emergence of a secondary plateau has been observed and studied [48, 58]. Since pre-ramp features have been linked to nearly conserved charges [59], it would be compelling to investigate whether the secondary plateau can be understood in terms of localized integrals of motion [77, 78].

Finally, our analysis can be extended to the sparse SYK model [72]. Notably, the adjacency matrix M introduced in Ref. [72] shares key properties with the matrix A in Eq. (2), such as the presence of a uniform eigenvector with eigenvalue 1. Investigating this connection further may provide insights into the transitions appearing as the sparsification rate increases.

Acknowledgements.—We would like to thank Gopal Chandra Santra, David Pascual Solis, Neil Talwar and Alex Windey for interesting discussions. This work was supported by the Swiss State Secretariat for Education, Research and Innovation (SERI) under contract number UeMO19-5.1; the Ministry of University and Research through FARE grant for the project DAVNE (Grant R20PEX7Y3A), and through project DYNAMITE QUANTERA2.00056, in the frame of ERANET COFUND QuantERA II – 2021 call co-funded by the European Union (H2020, GA No 101017733); the European Union - Next Generation EU, Mission 4, Component 2 - CUP E53D23002240006; the Provincia Autonoma di Trento, and Q@TN, the joint lab between University of Trento, FBK—Fondazione Bruno Kessler, INFN—National Institute for Nuclear Physics, and CNR—National Research Council. S.B. acknowledges CINECA for the use of HPC resources under ISCRAC projects ISSYK-2 (HP10CP8XXF) and DISYK (HP10CGNZG9).

* andrea.legramandi@unitn.it
 † soumik.bandyopadhyay@unitn.it
 ‡ philipp.hauke@unitn.it

- [1] A. Kitaev, “A simple model of quantum holography,” Talks given at “Entanglement in Strongly-Correlated Quantum Matter,” (Part 1, Part 2), KITP (2015).
- [2] S. Sachdev and J. Ye, *Phys. Rev. Lett.* **70**, 3339 (1993).
- [3] S. Sachdev, *Phys. Rev. X* **5**, 041025 (2015).

- [4] K. Jensen, *Phys. Rev. Lett.* **117**, 111601 (2016).
- [5] S. A. Hartnoll, A. Lucas, and S. Sachdev, *Holographic Quantum Matter* (The MIT Press, 2018).
- [6] D. Chowdhury, A. Georges, O. Parcollet, and S. Sachdev, *Rev. Mod. Phys.* **94**, 035004 (2022).
- [7] J. Maldacena and D. Stanford, *Phys. Rev. D* **94**, 106002 (2016).
- [8] I. Danshita, M. Hanada, and M. Tezuka, *Prog. Theor. Exp. Phys.* **2017**, 083101 (2017).
- [9] D. I. Pikulin and M. Franz, *Phys. Rev. X* **7**, 031006 (2017).
- [10] L. García-Álvarez, I. L. Egusquiza, L. Lamata, A. del Campo, J. Sonner, and E. Solano, *Phys. Rev. Lett.* **119**, 040501 (2017).
- [11] A. Chew, A. Essin, and J. Alicea, *Phys. Rev. B* **96**, 121119 (2017).
- [12] R. Babbush, D. W. Berry, and H. Neven, *Phys. Rev. A* **99**, 040301 (2019).
- [13] A. Chen, R. Ilan, F. de Juan, D. I. Pikulin, and M. Franz, *Phys. Rev. Lett.* **121**, 036403 (2018).
- [14] Z. Luo, Y.-Z. You, J. Li, C.-M. Jian, D. Lu, C. Xu, B. Zeng, and R. Laflamme, *Npj Quantum Inf.* **5**, 53 (2019).
- [15] C. Wei and T. A. Sedrakyan, *Phys. Rev. A* **103**, 013323 (2021).
- [16] P. Uhrich, S. Bandyopadhyay, N. Sauerwein, J. Sonner, J.-P. Brantut, and P. Hauke, [arXiv:2303.11343 \[quant-ph\]](https://arxiv.org/abs/2303.11343) (2023), [10.48550/arXiv.2303.11343](https://arxiv.org/abs/10.48550/arXiv.2303.11343).
- [17] R. Baumgartner, P. Pelliconi, S. Bandyopadhyay, F. Orsi, N. Sauerwein, P. Hauke, J.-P. Brantut, and J. Sonner, (2024), [arXiv:2411.17802 \[quant-ph\]](https://arxiv.org/abs/2411.17802).
- [18] J. W. Britton, B. C. Sawyer, A. C. Keith, C.-C. J. Wang, J. K. Freericks, H. Uys, M. J. Biercuk, and J. J. Bollinger, *Nature* **484**, 489 (2012).
- [19] P. Jurcevic, B. P. Lanyon, P. Hauke, C. Hempel, P. Zoller, R. Blatt, and C. F. Roos, *Nature* **511**, 202 (2014).
- [20] J. Smith, A. Lee, P. Richerme, B. Neyenhuis, P. W. Hess, P. Hauke, M. Heyl, D. A. Huse, and C. Monroe, *Nat. Phys.* **12**, 907 (2016).
- [21] N. Trautmann and P. Hauke, *Phys. Rev. A* **97**, 023606 (2018).
- [22] L. Chomaz, I. Ferrier-Barbut, F. Ferlaino, B. Laburthe-Tolra, B. L. Lev, and T. Pfau, *Rep. Prog. Phys.* **86**, 026401 (2022).
- [23] A. Browaeys and T. Lahaye, *Nat. Phys.* **16**, 132 (2020).
- [24] S. L. Cornish, M. R. Tarbutt, and K. R. A. Hazzard, *Nature Physics* **20**, 730 (2024).
- [25] D. D. Awschalom, R. Hanson, J. Wrachtrup, and B. B. Zhou, *Nature Photonics* **12**, 516 (2018).
- [26] X. Chen and T. Zhou, *Phys. Rev. B* **100**, 064305 (2019).
- [27] A. L. Burin, *Phys. Rev. B* **91**, 094202 (2015).
- [28] A. L. Burin, *Phys. Rev. B* **92**, 104428 (2015).
- [29] P. Hauke and M. Heyl, *Phys. Rev. B* **92**, 134204 (2015).
- [30] K. S. Tikhonov and A. D. Mirlin, *Phys. Rev. B* **97**, 214205 (2018).
- [31] X. Deng, V. E. Kravtsov, G. V. Shlyapnikov, and L. Santos, *Phys. Rev. Lett.* **120**, 110602 (2018).
- [32] S. J. Thomson and M. Schiró, *Phys. Rev. Res.* **2**, 043368 (2020).
- [33] X. Deng, S. Ray, S. Sinha, G. V. Shlyapnikov, and L. Santos, *Phys. Rev. Lett.* **123**, 025301 (2019).
- [34] S. Nag and A. Garg, *Phys. Rev. B* **99**, 224203 (2019).
- [35] S. Roy and D. E. Logan, *SciPost Phys.* **7**, 042 (2019).
- [36] X. Deng, G. Masella, G. Pupillo, and L. Santos, *Phys. Rev. Lett.* **125**, 010401 (2020).
- [37] R. Modak and T. Nag, *Phys. Rev. Res.* **2**, 012074 (2020).
- [38] R. Modak and T. Nag, *Phys. Rev. E* **101**, 052108 (2020).
- [39] C. Cheng, *Phys. Rev. B* **108**, 155113 (2023).
- [40] A. D. Mirlin, Y. V. Fyodorov, F.-M. Dittes, J. Quezada, and T. H. Seligman, *Phys. Rev. E* **54**, 3221 (1996).
- [41] P. W. Anderson, *Phys. Rev.* **109**, 1492 (1958).
- [42] M. JANSSEN, *Int. J. Mod. Phys. B* **08**, 943–984 (1994).
- [43] F. Evers and A. D. Mirlin, *Rev. Mod. Phys.* **80**, 1355 (2008).
- [44] Y. V. Fyodorov and A. D. Mirlin, *Phys. Rev. Lett.* **67**, 2405 (1991).
- [45] E. Brézin and S. Hikami, *Phys. Rev. E* **55**, 4067 (1997).
- [46] P. Saad, S. H. Shenker, and D. Stanford, (2018), [arXiv:1806.06840 \[hep-th\]](https://arxiv.org/abs/1806.06840).
- [47] P. Kos, M. Ljubotina, and T. Prosen, *Phys. Rev. X* **8**, 021062 (2018), [arXiv:1712.02665 \[nlín.CD\]](https://arxiv.org/abs/1712.02665).
- [48] H. Gharibyan, M. Hanada, S. H. Shenker, and M. Tezuka, *J. High Energ. Phys.* **2018**, 124 (2018).
- [49] A. Chan, A. De Luca, and J. T. Chalker, *Phys. Rev. Lett.* **122**, 220601 (2019).
- [50] J. Šuntajs, J. Bonča, T. Prosen, and L. Vidmar, *Phys. Rev. E* **102**, 062144 (2020), [arXiv:1905.06345 \[cond-mat.str-el\]](https://arxiv.org/abs/1905.06345).
- [51] Nivedita, H. Shackleton, and S. Sachdev, *Phys. Rev. E* **101**, 042136 (2020).
- [52] R. Prakash and A. Lakshminarayanan, *Phys. Rev. B* **101**, 121108 (2020).
- [53] A. Prakash, J. H. Pixley, and M. Kulkarni, *Phys. Rev. Res.* **3**, L012019 (2021).
- [54] J. Šuntajs, T. Prosen, and L. Vidmar, *Annals of Physics* **435**, 168469 (2021), special issue on Philip W. Anderson.
- [55] D. K. Nandy, T. Čadež, B. Dietz, A. Andreanov, and D. Rosa, *Phys. Rev. B* **106**, 245147 (2022).
- [56] T. Anegawa, N. Iizuka, A. Mukherjee, S. K. Sake, and S. P. Trivedi, *JHEP* **11**, 234 (2023), [arXiv:2305.07505 \[hep-th\]](https://arxiv.org/abs/2305.07505).
- [57] R. Barney, M. Winer, C. L. Baldwin, B. Swingle, and V. Galitski, *SciPost Phys.* **15**, 084 (2023).
- [58] M. Hopjan and L. Vidmar, *Phys. Rev. Res.* **5**, 043301 (2023).
- [59] R. L. Baumgartner, L. V. Delacrétaz, P. Nayak, and J. Sonner, (2024), [arXiv:2405.19260 \[cond-mat.stat-mech\]](https://arxiv.org/abs/2405.19260).
- [60] P. Orman, H. Gharibyan, and J. Preskill, (2024), [arXiv:2403.13884 \[hep-th\]](https://arxiv.org/abs/2403.13884).
- [61] W. Buijsman, *Phys. Rev. B* **109**, 024205 (2024).
- [62] H. Dong, P. Zhang, C. B. Dag, Y. Gao, N. Wang, J. Deng, X. Zhang, J. Chen, S. Xu, K. Wang, Y. Wu, C. Zhang, F. Jin, X. Zhu, A. Zhang, Y. Zou, Z. Tan, Z. Cui, Z. Zhu, F. Shen, T. Li, J. Zhong, Z. Bao, H. Li, Z. Wang, Q. Guo, C. Song, F. Liu, A. Chan, L. Ying, and H. Wang, (2024), [arXiv:2403.16935 \[quant-ph\]](https://arxiv.org/abs/2403.16935).
- [63] M. Winer, S.-K. Jian, and B. Swingle, *Phys. Rev. Lett.* **125**, 250602 (2020).
- [64] Y. Liao, A. Vikram, and V. Galitski, *Phys. Rev. Lett.* **125**, 250601 (2020).
- [65] W.-F. Xu and W. J. Rao, *Sci. Rep.* **13**, 634 (2023).
- [66] V. E. Kravtsov and K. A. Muttalib, *Phys. Rev. Lett.* **79**, 1913 (1997).
- [67] F. Evers and A. D. Mirlin, *Phys. Rev. Lett.* **84**, 3690 (2000).
- [68] I. Varga and D. Braun, *Phys. Rev. B* **61**, R11859 (2000).

- [69] A. D. Mirlin and F. Evers, *Phys. Rev. B* **62**, 7920 (2000).
 [70] E. Bogomolny and M. Sieber, *Phys. Rev. E* **98**, 042116 (2018).
 [71] P. A. Nosov, I. M. Khaymovich, and V. E. Kravtsov, *Phys. Rev. B* **99**, 104203 (2019).
 [72] S. Xu, L. Susskind, Y. Su, and B. Swingle, [arXiv:2008.02303](https://arxiv.org/abs/2008.02303) [*cond-mat.str-el*] (2020), 10.48550/arXiv.2008.02303.
 [73] See *supplemental material*.
 [74] In [73] we discuss further motivation for this assumption coming from an analysis of A eigenvalues: since most of the vanishes in the thermodynamic limit, they lead to a vanishing Fourier components of Σ , forcing the solution to be uniform.
 [75] Since we are interested in the $N \rightarrow \infty$ limit, we preferred using an intuitive but less precise notation that does not distinguish between even and odd N .
 [76] A. Legramandi and T. Neil, To Appear.
 [77] M. Serbyn, Z. Papić, and D. A. Abanin, *Phys. Rev. Lett.* **111**, 127201 (2013).
 [78] D. A. Huse, R. Nandkishore, and V. Oganesyan, *Phys. Rev. B* **90**, 174202 (2014).
 [79] This is a consequence of the fact that v_1 is an eigenvalue also for A^{-1} with eigenvector $\lambda_1^{-1} = \mathcal{N}^{-2}$.
 [80] A. Kamenev and M. Mézard, *Phys. Rev. B* **60**, 3944 (1999).

SUPPLEMENTAL MATERIAL

In this supplemental material, we provide detailed explanations and derivations to complement the calculations presented in the main text. In Section A, we show some intermediate steps in the derivation of Eq. (5) and discuss how to recover the $\alpha = 0$ case, corresponding to the quadratic SYK model discussed in Ref. [63]. Section B contains a detailed analysis of the symmetries of the saddle-point equation and a discussion of its solutions. In Section C, we derive the explicit form of the eigenvalues of the matrix A in the $N \rightarrow \infty$ limit. Sections D and E focus on the calculation of the spectral form factor (SFF) up to the 1-loop level. These contributions are particularly important at late times, where the classical action vanishes. In Section D, we analyze time-translation-invariant fluctuations, including the zero modes responsible for the ramp. Section E incorporates the leading contribution from the soft modes. By combining these contributions with the classical action, which dominates at early times, we derive in Section F an analytic expression for the SFF, used in the main text for comparison with numerical results. In Section G, we go beyond the 1-loop terms to explore perturbative corrections to the classical saddle points with respect to time-translation-invariant configurations. This calculation demonstrates that the perturbative series becomes ill-defined for $\alpha > 1/2$. Finally, in Section H, we provide details on the numerical methods employed in the main text.

A. Path integral for the spectral form factor and $\alpha = 0$ case

In this section we show some details about the path integral calculation presented in the main text and explain how to consistently take the $\alpha \rightarrow 0$ limit in the hopping terms (1) to recover the quadratic SYK model. The starting point of this section is the expression of the spectral form factor (SFF), Eq. (4) of the main text, which can be more explicitly written as

$$g(T) = \int \mathcal{D}\psi^L \mathcal{D}\psi^R \left\langle \exp \left\{ - \sum_{i=1}^N \int_0^T dt \left(\frac{1}{2} \psi^L \partial_t \psi^L + \frac{1}{2} \psi^R \partial_t \psi^R + \sum_{j=i+1}^N \frac{J_{ij}}{\mathcal{N}} a_{ij} (\psi_i^L \psi_j^L - \psi_i^R \psi_j^R) \right) \right\} \right\rangle. \quad (\text{S1})$$

From here, it is straightforward to perform the Gaussian integral over the couplings, which leads to the following expression:

$$g(T) = \int \mathcal{D}\psi^L \mathcal{D}\psi^R \exp \left\{ - \sum_{i=1}^N \int_0^T dt \frac{1}{2} (\psi^L \partial_t \psi^L + \psi^R \partial_t \psi^R) - \frac{J^2}{2\mathcal{N}^2} \sum_{j=i+1}^N a_{ij}^2 \left(\int_0^T dt (\psi_i^L \psi_j^L - \psi_i^R \psi_j^R) \right)^2 \right\}, \quad (\text{S2})$$

To find the saddle-point solution, one typically introduces a two-point function field corresponding to the fermionic correlator [7]. As mentioned in the body of the paper, differently from the usual SYK case, for our purposes this two-point function field cannot be spatially averaged, since local fields are needed to keep account of the spatial envelope. We thus use the identity

$$1 = \prod_i \int \mathcal{D}G_i \delta(G_i^{ab}(t, t') - \psi_i^a(t) \psi_i^b(t')) = \prod_i \int \mathcal{D}G_i \mathcal{D}\Sigma_i \exp \left\{ \frac{i}{2} \sum_{a,b} \iint_0^T dt dt' \Sigma_i^{ab}(t, t') (G_i^{ab}(t, t') - \psi_i^a(t) \psi_i^b(t')) \right\}. \quad (\text{S3})$$

Notice that the way we introduced G and Σ implies the following relations:

$$G_i^{ab}(t_1, t_2) = -G_i^{ba}(t_2, t_1) = G_i^{ba}(t_2, t_1)^*, \quad \Sigma_i^{ab}(t_1, t_2) = -\Sigma_i^{ba}(t_2, t_1) = \Sigma_i^{ba}(t_2, t_1)^*. \quad (\text{S4})$$

Plugging this expression into the SFF and expanding the square term, we can replace the fermions with G_i , yielding

$$g(T) = \int \mathcal{D}\psi^a \mathcal{D}G_i \mathcal{D}\Sigma_i \exp \left\{ -\frac{1}{2} \sum_{i=1}^N \sum_{ab} \iint_0^T dt dt' \left[\left(\psi_i^a(t) (\delta(t-t') \delta_{ab} \partial_{t'} - i \Sigma_i^{ab}(t, t')) \psi_i^b(t') \right) \right. \right. \\ \left. \left. - i \Sigma_i^{ab}(t, t') G_i^{ab}(t, t') + \frac{J^2}{2} (-)^{a+b} \sum_{j \neq i}^N A_{ij} G_i^{ab}(t, t') G_j^{ab}(t, t') \right] \right\}, \quad (\text{S5})$$

where we also used $A_{ij} = A_{ji}$.

From here, it is now instructive to discuss how one can obtain the usual SYK₂ spectral from factor [63] at $\alpha \rightarrow 0$. The main difference so far in the $\alpha \rightarrow 0$ limit with respect to usual SYK₂, is how the propagators have been introduced in Eq. (S3), namely, as mentioned above, as a product of two Majorana spinors on a single site instead of averaging over all the positions. Another subtle point is that we are setting $i \neq j$ in the summation over j . These points are actually related: the standard SYK literature [7, 46] usually takes advantage of the fact that for the Grassmannian variables we have $\psi_j \psi_j = 0$, permitting one to extend the sum also to $j = i$. This would correspond in our case to setting $A_{ii} = 1/\mathcal{N}^2$ instead of Eq. (2). We have not done that, since we would have also needed to enforce the constraint $G_i(t, t_1) G_i(t, t_2) = 0$. For the purpose of this section, it is useful to set $A_{ii} = 1/\mathcal{N}^2$ in order to exactly recover the usual SYK case. The discussion that follows holds also for $A_{ii} = 0$ up to $1/N$ corrections.

By following the above convention, we now have $A_{ij}(\alpha = 0) = 1/\mathcal{N}^2$ for all i, j , and therefore A is a degenerate matrix with the single non-vanishing eigenvector

$$v_0 = \frac{1}{\sqrt{N}}(1 \dots 1), \quad (\text{S6})$$

corresponding to the eigenvalue $\lambda_0 = 1$. We call v_k with $k \neq 0$ the basis vectors that span the remaining degenerate subspace of A . To evaluate the path integral, it is convenient to use this basis, in which the propagator reads

$$\hat{G}_0^{ab} = \frac{(G_1^{ab}, \dots, G_N^{ab}) \cdot v_0}{\sqrt{N}} = \frac{1}{N} \sum_i G_i^{ab}, \quad \hat{G}_k^{ab} = (G_1^{ab} \dots G_N^{ab}) \cdot v_k. \quad (\text{S7})$$

Here, we have added a factor \sqrt{N} simply to make the notation consistent with the one usually used in the context of the standard SYK.

After these manipulations and using $\mathcal{N}(\alpha = 0)^2 = N$, the SFF reads

$$g(T) = \int \mathcal{D}\psi^a \mathcal{D}G_i \mathcal{D}\Sigma_i \exp \left\{ -\frac{1}{2} \sum_{ab} \int_0^T dt dt' \left[\sum_{i=1}^N \left(\psi_i^a(t) (\delta(t-t') \delta_{ab} \partial_{t'} - i \Sigma_i^{ab}(t, t')) \psi_i^b(t') \right) \right. \right. \\ \left. \left. - i \sqrt{N} \hat{\Sigma}_0^{ab}(t, t') \hat{G}_0^{ab}(t, t') - i \sum_{k \neq 0} \hat{\Sigma}_k^{ab}(t, t') \hat{G}_k^{ab}(t, t') + \frac{J^2 N}{2} (-)^{a+b} \hat{G}_0^{ab}(t, t')^2 \right] \right\}. \quad (\text{S8})$$

This expression is linear in the propagators \hat{G}_k^{ab} , allowing us to integrate them out. The result of this integration will produce some delta functions $\delta(\hat{\Sigma}_k)$. Since $\{v_k\}$ span an orthonormal basis, we must have $v_0 \cdot v_k = 0$ for all $k \neq 0$, meaning that the degenerate subspace of A is spanned by vectors whose components sum to zero. This implies that these delta functions can be re-organized as

$$\prod_{k \neq 0} \delta(\hat{\Sigma}_k) = \prod_{k \neq 0} \delta \left(\sum_i \Sigma_i^{ab} (v_k)_i \right) = N \prod_{i > 1} \delta(\Sigma_1^{ab} - \Sigma_i^{ab}). \quad (\text{S9})$$

If we now call $\Sigma^{ab} = \hat{\Sigma}_1^{ab}$ and $G^{ab} = \hat{G}_0^{ab}$, we exactly retrieve the familiar expression of the standard SYK₂ model [63],

$$g(T) = \int \mathcal{D}\psi^a \mathcal{D}G \mathcal{D}\Sigma \exp \left\{ -\frac{1}{2} \sum_{ab} \int_0^T dt dt' \left[\sum_{i=1}^N \left(\psi_i^a(t) (\delta(t-t') \delta_{ab} \partial_{t'} - i \Sigma^{ab}(t, t')) \psi_i^b(t') \right) \right. \right. \\ \left. \left. - i N \Sigma^{ab}(t, t') G^{ab}(t, t') + \frac{J^2 N}{2} (-)^{a+b} G^{ab}(t, t')^2 \right] \right\}. \quad (\text{S10})$$

Before concluding this section, let us briefly discuss how one can take the $\alpha \rightarrow 0$ limit after the integration of the fermions and the G_i , i.e., from Eq. (5). For doing so, it is important to impose a normalization for the path integral. Following Ref. [63], we divide with respect to the same integral but with the Gaussian part only, i.e., without the $\text{Tr} \log$ term. The idea is that the Gaussian part dominates in the interaction-less case $J \rightarrow 0$, and, since JT is the only dimensionless quantity, this renormalization also imposes $g(0) = 1$. Moreover, this choice becomes important when we want to recover the $\alpha = 0$ limit. Indeed, the matrix A_{ij}^{-1} in this case is not defined due to infinite eigenvalues. However, thanks to the normalization, we have that the path integral is not diverging and the Gaussian terms with infinite eigenvalues approach Dirac delta functions as the ones in Eq. (S9), giving the same results as in Ref. [63].

B. Symmetries and solutions to the saddle point equation

In this section, we discuss the symmetries and some manipulations of the saddle point equation (6). First of all, it is convenient to re-write it in matrix form with respect to the replica indices ab ,

$$\sum_j A_{ij}^{-1}(\omega_n \mathbf{1} - \Sigma_i(\omega_n)) \sigma_3 \Sigma_j^t(-\omega_n) \sigma_3 = -J^2. \quad (\text{S11})$$

Second, Eq. (S4) implies that $\Sigma_i(\omega_n) = \Sigma_i(\omega_n)^\dagger$. A natural way for a symmetry to act on Σ is through the adjoint action $\Sigma_i(\omega_n) \rightarrow U_i(\omega_n) \Sigma_i(\omega_n) U_i(\omega_n)^{-1}$. Since we want the transformed Σ to be hermitian, we have to require that $U_i(\omega_n)$ is a representation of the special unitary group $\text{SU}(2)$. To have an actual symmetry, we must impose two more constraints, the first one is that $U_i(\omega_n)$ is site independent (for this reason from now on we will drop the subscript i). The second condition is a relation between the positive and negative frequencies, which transform in a different but correlated way, so that just one of them is really independent. If we fix $\omega_n > 0$, we find the following transformation rules

$$\Sigma_i(\pm\omega_n) \rightarrow U(\pm\omega_n) \Sigma_i(\pm\omega_n) U(\pm\omega_n)^{-1}, \quad U(-\omega_n) = \sigma_3 U(\omega_n)^* \sigma_3. \quad (\text{S12})$$

Notice that for each positive Matsubara frequency we have an independent $\text{SU}(2)$ transformation, leading to an effectively infinite dimensional symmetry group.

Now, we will discuss how to get the saddle point solution Eq. (7). In order to make progress with Eq. (6), we use the conditions of Eq. (S4), which implies $\Sigma_i^{ba}(-\omega_n) = -\Sigma_i^{ab}(\omega_n)$, to write Eq. (6) in terms of just one frequency:

$$\frac{1}{J^2} \sum_j A_{ij}^{-1} \Sigma_j^{ab}(\omega_n) = (-)^{a+b} (\omega_n \delta^{ab} - \Sigma_i^{ab}(\omega_n))^{-1}. \quad (\text{S13})$$

Now, we perform a Fourier transform of the equation above along the spatial direction, so that we can diagonalize the matrix A_{ij}^{-1} , as shown in the next section. The result of this operation is

$$\hat{\Sigma}_{-k}^{ab}(\omega_n) = \lambda_k J^2 (-)^{a+b} \widehat{(\omega_n \delta^{ab} - \Sigma^{ab}(\omega_n))^{-1}}_k, \quad (\text{S14})$$

where λ_k are the eigenvalues of A , while the hat indicates the Fourier transform. From the exact expression of the eigenvalues given in section C, we know that, for $\alpha \sim 0$ we have $\lambda_0 = 1$ and $\lambda_{k \neq 0} \sim 0$, which implies that $\Sigma_{k \neq 0} \sim 0$. Therefore, for $\alpha \sim 0$ we have a single non-vanishing solution, which is independent of the site position. In the main text, we have assumed that this saddle dominates at least up to $\alpha = 1/2$. This assumption is justified by the fact that for α small most of the eigenvalues are very close to zero. However, for $\alpha > 1/2$ the situation changes, and we have that most of the eigenvalues are non-zero.

By setting $\Sigma_i^{ab} = \tilde{\Sigma}^{ab}$ and noticing that $\sum_j A_{ij}^{-1} = \mathcal{N}^{-2}$ [79], we get

$$\frac{1}{J^2} \tilde{\Sigma}^{ab}(\omega_n) = (-)^{a+b} (\omega_n \delta^{ab} - \tilde{\Sigma}^{ab}(\omega_n))^{-1}. \quad (\text{S15})$$

This equation can be easily solved and the dominant saddle is given in Eq. (7).

C. More details on the eigenvalues in the thermodynamic limit

In this section, we give some more details on the derivation of the eigenvalues of A , for arbitrary α . For calculating them it is convenient to perform a Fourier transform and go to momentum space. In the following, we will suppress

the time and L, R indices in order to make the notation lighter and we will assume that N is odd, which will not affect the result in the large N limit:

$$\begin{aligned}
\sum_{i,j} A_{ij} G_i G_j &= \frac{1}{N} \sum_{k,p} \sum_{ij} A_{ij} e^{i \frac{2\pi}{N} (ik+jp)} \hat{G}_k \hat{G}_p \\
&= \frac{1}{N\mathcal{N}} \sum_{k,p} \sum_{i=1}^N \sum_{\Delta=-\lfloor N/2 \rfloor}^{\lfloor N/2 \rfloor} \frac{e^{i \frac{2\pi}{N} (i(k+p))} e^{i \frac{2\pi}{N} \Delta k}}{|\Delta|^{2\alpha}} \hat{G}_k \hat{G}_p \\
&= \sum_k \left(\frac{1}{\mathcal{N}} \sum_{\Delta=-\lfloor N/2 \rfloor}^{\lfloor N/2 \rfloor} \frac{e^{i \frac{2\pi}{N} \Delta k}}{|\Delta|^{2\alpha}} \right) \hat{G}_k \hat{G}_{-k},
\end{aligned} \tag{S16}$$

where we have introduced in the second step the distance between two sites $\Delta = i - j$, the floor function $\lfloor \bullet \rfloor$ and we defined the Fourier transform as

$$\hat{G}_k = \frac{1}{\sqrt{N}} \sum_{i=-\lfloor N/2 \rfloor}^{\lfloor N/2 \rfloor} e^{i \frac{2\pi}{N} ik} G_i. \tag{S17}$$

With this, the eigenvalues of A_{ij} can be read from the term in the parenthesis of Eq. (S16), and are

$$\lambda_k = \frac{1}{\mathcal{N}} \sum_{\Delta=-\lfloor N/2 \rfloor}^{\lfloor N/2 \rfloor} \frac{e^{i \frac{2\pi}{N} \Delta k}}{|\Delta|^{2\alpha}} = \frac{\sum_{\Delta=1}^{\lfloor N/2 \rfloor} \Delta^{-2\alpha} \cos\left(\frac{2\pi}{N} \Delta k\right)}{\sum_{\Delta=1}^{\lfloor N/2 \rfloor} \Delta^{-2\alpha}}. \tag{S18}$$

as in Eq. (12). In principle, since A is a symmetric real matrix, we could have diagonalize it also by using an orthogonal change of coordinate. This is defined by:

$$G_j = \sqrt{\frac{1}{N}} \hat{G}_0 + \sqrt{\frac{2}{N}} \sum_{k>0} \left[\cos\left(\frac{2\pi}{N} ik\right) \hat{G}_k - \sin\left(\frac{2\pi}{N} ik\right) \hat{G}_{-k} \right]. \tag{S19}$$

The next step is to take the thermodynamic limit. For $\alpha < 1/2$, \mathcal{N} is divergent while the rest of the expression is finite, which leads to a vanishing contribution. For $\alpha > 1/2$ \mathcal{N} becomes convergent can now define $\tilde{k} = \frac{2\pi}{N} k$ with $-\pi < \tilde{k} < \pi$ to get the result in (13).

Now, let us give some more details about the derivation of Eq. (14). The starting point is the finite- N expression (12), from which we proceed by expanding the cosine in a power series:

$$\begin{aligned}
\lambda_k &= \frac{\sum_{\Delta=1}^{\lfloor N/2 \rfloor} \Delta^{-2\alpha} \cos\left(\frac{2\pi}{N} \Delta k\right)}{\sum_{\Delta=1}^{\lfloor N/2 \rfloor} \Delta^{-2\alpha}} \\
&= \frac{\sum_{n=0}^{\infty} \frac{(-1)^n}{2n!} \left(\frac{2\pi}{N} k\right)^{2n} \sum_{\Delta=1}^{\lfloor N/2 \rfloor} \Delta^{2n-2\alpha}}{\sum_{\Delta=1}^{\lfloor N/2 \rfloor} \Delta^{-2\alpha}} \\
&= 1 + \sum_{n=1}^{\infty} \frac{(-1)^n}{2n!} (2\pi k)^{2n} \frac{1}{N^{2n}} \frac{\sum_{\Delta=1}^{\lfloor N/2 \rfloor} \Delta^{2n-2\alpha}}{\sum_{\Delta=1}^{\lfloor N/2 \rfloor} \Delta^{-2\alpha}}.
\end{aligned} \tag{S20}$$

For finite k , it is possible to take the $N \rightarrow \infty$ limit of the term in the last term alone,

$$\lim_{N \rightarrow \infty} \frac{1}{N^{2n}} \frac{\sum_{\Delta=1}^{\lfloor N/2 \rfloor} \Delta^{2n-2\alpha}}{\sum_{\Delta=1}^{\lfloor N/2 \rfloor} \Delta^{-2\alpha}} = \begin{cases} 4^{-n} \frac{1-2\alpha}{1-2(\alpha-n)} & \alpha \leq 1/2 \\ 0 & \alpha > 1/2. \end{cases} \tag{S21}$$

By plugging this expression back into the summation, one obtains the result in Eq. (14). Notice that all the λ_k , as a function of α , are continuous, but they are not smooth at $\alpha = 1/2$.

D. Analytic calculation of the ramp

In this section we calculate the leading contribution to the path integral which is responsible for the exponential ramp. We slightly change our conventions in order to follow the notation of the Supplemental Material of Ref. [63],

so that the interested reader to better compare our results to the ones in Ref. [63], which can be recovered in the $\alpha \rightarrow 0$ limit. The same notation will be used in section G. This convention uses a slightly different but equivalent Hamiltonian for the R action, namely

$$\mathcal{H}_R = -\frac{i}{\mathcal{N}} \sum_{i < j}^N J_{ij} a_{ij} \psi_i^R \psi_j^R, \quad (\text{S22})$$

which allows us to get rid of the $(-)^{a+b}$ term in Eq. (S5). Moreover, we also absorb an i in the definition of Σ , which sends $\Sigma \rightarrow -i\Sigma$. After these notational changes, the SFF reads

$$g(T) = \int \mathcal{D}\Sigma_i \exp \left\{ \frac{1}{2} \sum_i \text{Tr} \log(\delta(t-t') \delta_{ab} \partial_{t'} - \Sigma_i^{ab}(t, t')) + \frac{\mathcal{N}^2}{4J^2} \sum_{abj} \int_0^T dt dt' A_{ij}^{-1} \Sigma_i^{ab}(t, t') \Sigma_j^{ab}(t, t') \right\}. \quad (\text{S23})$$

To analyze the leading contribution to the exponential ramp, we assume time-translation invariance, expressed as $\Sigma_i^{ab}(t, t') = \Sigma_i^{ab}(t - t')$. This assumption effectively captures the semiclassical saddle point and the zero modes relevant to the ramp. However, it does not account for the massive modes that govern the late-time behavior of the ramp and the eventual transition to the plateau, which require a separate discussion (see section E). The time-invariance symmetry makes it convenient to Fourier transform into frequency space. We also define the dimensionless quantities $(\sigma_n^i)^{ab} = \Sigma_i^{ab}(\omega_n)/J$ and $x_n = \omega_n/J$, where σ_n^i is a Hermitian two-dimensional matrix. The SFF for the time-translation invariant (t.t.i.) configurations can be expressed as an infinite product of finite dimensional integrals,

$$g^{\text{t.t.i.}}(T) = \prod_{n > 0} g_n(T) \quad g_n(T) = \frac{\int d\sigma_n^i e^{I[\sigma_n^i]}}{\pi^{2N} \det(A/\mathcal{N})^2}, \quad (\text{S24})$$

$$I[\sigma_n] = \sum_i \frac{1}{2} \text{Tr} \log \left[\left(1 - i \frac{\sigma_n^i}{x_n} \right) \left(1 - i \frac{\sigma_n^i}{x_n} \right)^t \right] - \frac{\mathcal{N}^2}{2} \sum_{i,j} A_{ij}^{-1} \text{Tr}(\sigma_n^i \sigma_n^j), \quad (\text{S25})$$

where we used $\sigma_{-n}^i = (\sigma_n^i)^T$ for multiplying the positive and negative contributions together and thus restrict the product to $n > 0$. Each integral is already normalized with the same normalization discussed in section A.

The dominant saddle points are the same as those given by Eq. (7), up to the change of conventions:

$$\tilde{\sigma}_n = \begin{cases} -\frac{i}{2}(x_n - \sqrt{x_n^2 - 4}) & x_n > 2, \\ -\frac{i}{2}(x_n - i\sqrt{4 - x_n^2}\sigma_3) & x_n < 2. \end{cases} \quad (\text{S26})$$

The saddle point action can be obtained by evaluating $I[\tilde{\sigma}_n]$ and has been explicitly computed in Ref. [63]:

$$I[\tilde{\sigma}_n] = \begin{cases} N \left[\log \left(\frac{1}{2} \left(1 + \sqrt{1 - \frac{4}{x_n^2}} \right) - \frac{1}{x_n^2} \right) + \frac{x_n}{4} \left(1 - \sqrt{1 - \frac{4}{x_n^2}} \right)^2 \right] & x_n > 2, \\ N \left[-\log x_n^2 + \frac{1}{2}(x_n^2 - 2) \right] & x_n < 2. \end{cases} \quad (\text{S27})$$

To include the contribution beyond the saddle point approximation, we have to expand the fields in the fluctuations around it

$$\sigma_n = \tilde{\sigma}_n + \delta\sigma_n, \quad I[\tilde{\sigma}_n + \delta\sigma_n] = I[\tilde{\sigma}_n] + \delta I_n[\delta\sigma_n], \quad (\text{S28})$$

where we chose a basis for the fluctuation $\delta\sigma_n$ that already diagonalizes the matrix A , so that the the quadratic action reads

$$\delta I_n^{(2)} = -\frac{1}{2} \sum_k \text{Tr} (\tilde{\sigma}_n \delta\sigma_n^k \tilde{\sigma}_n \delta\sigma_n^k) - \frac{1}{\lambda_k} \text{Tr}(\delta\sigma_n^k \delta\sigma_n^k). \quad (\text{S29})$$

A convenient way for performing the integral over $\delta\sigma_n^k$ is to expand it on the Pauli matrix basis,

$$\delta\sigma_n^k = \sum_{\mu} y_{\mu}^k \sigma_{\mu}, \quad (\text{S30})$$

where $\sigma_4 = 1$. In these new coordinates

$$\delta I_n^{(2)} = - \sum_k \left(\tilde{\sigma}_n^{LL} \tilde{\sigma}_n^{RR} ((y_1^k)^2 + (y_2^k)^2) + \frac{\tilde{\sigma}_n^{RR}}{2} ((y_3^k)^2 - (y_2^k)^4) + \frac{\tilde{\sigma}_n^{LL}}{2} ((y_3^k)^2 + (y_2^k)^4) + \frac{1}{\lambda_i} ((y_1^k)^2 + (y_2^k)^2 + (y_3^k)^2 + (y_4^k)^2) \right). \quad (\text{S31})$$

Due to the form of the saddle point solution (S26), it is convenient to split the calculation in two pieces, depending on whether $x_n \gtrless 2$. For $x_n < 2$ it is possible to explicitly notice that we have zero modes corresponding and $k = 0$, which are due to the fact that $\lambda_0 = 1$ and $\tilde{\sigma}_n^{LL} \tilde{\sigma}_n^{RR} = -1$. A naive integration of (S31) over $y_{1,2}^0$ would therefore lead to a divergent result, since the variables seem to run over the real axis. However, these zero-modes are generated by the degeneracy of the symmetry broke saddle-point solution, which means that $y_{1,2}^0$ can only explore the null directions, which, as discussed in [80], are restricted to the saddle point manifold $\text{SU}(2)/\text{U}(1)$. This means that the integral over the Goldstone modes just contributes as the vacuum-manifold volume:

$$\int dy_1^0 dy_2^0 = 4\pi N(1 - x_n^2/4). \quad (\text{S32})$$

Let us now break down this expression. The vacuum manifold is given by the coset space $\text{SU}(2)/\text{U}(1)$, which is a two-dimensional sphere. The volume of a two-dimensional sphere with radius r is given by $4\pi r^2$, so, we just need to understand what is r in our case. First of all, we point out that by rotating the fluctuations in such a way that $\delta\sigma_i$ diagonalizes A , we are going into the real basis defined in (S19). The eigenvector corresponding to $\lambda_0 = 1$ is

$$\sigma_n^0 = \frac{1}{\sqrt{N}} \sum_i \sigma_n^i. \quad (\text{S33})$$

On the saddle point solution, we have that $\sigma_n^i = \tilde{\sigma}_n$, which means $\sigma_n^0 = \sqrt{N} \tilde{\sigma}_n$. Now, the radius of the vacuum manifold is given by the coefficient of the symmetry-breaking part of the saddle solution, which is the one proportional to σ_3 in Eq. (S26), so that we have $r = \sqrt{N(1 - x_n^2/4)}$, where we already include the \sqrt{N} dependence discussed before. This exactly reproduces the result in Eq. (S32)

The integral over the other coordinates $y_{3,4}^k$ in Eq. (S31) is a simple Gaussian integration. The overall result for $x_n < 2$ is:

$$g_n = e^{I[\tilde{\sigma}_n]} N \sqrt{4 - x_n^2} \prod_{k \neq 0} \frac{1}{(1 - \lambda_k) \sqrt{1 + \lambda_k(1 - x_n^2 + \lambda_k)}}. \quad (\text{S34})$$

This completes the calculation of the time-translation invariant part of the SFF up to the one-loop term for $x_n < 2$. As a sanity check of Eq. (S34), we can recover the $\alpha = 0$ case: from Eq. (S34) it is very simple to take the $\alpha \rightarrow 0$ limit, since, thanks to the path integral renormalization, the eigenvalues λ_k appear in a regular way in the final result. In the large N limit, this gives the same result as what we would have gotten directly from Ref. [63], since the product in Eq. (S34) collapses to 1 in this limit.

Now, we can analyze the one-loop calculation for $x_n > 2$. In this case, we do not have zero modes and we can simply perform the Gaussian integral of the quadratic action in Eq. (S31). The contributions to the SFF in this regime is given by

$$g_n = e^{I[\tilde{\sigma}_n]} \prod_k \left(1 + \frac{\lambda_k}{2} (2 - x_n^2 + x_n \sqrt{x_n^2 - 4}) \right)^{-2}. \quad (\text{S35})$$

The final expression of the one-loop contribution to the SFF for the time-translation invariant configurations as defined in Eq. (S24) is given by the product of the factors given by Eq. (S34) and Eq. (S35) over all the Matsubara frequencies. This expression can be explicitly evaluated at late time $JT \gg 1$. Neglecting the classical action terms (which give a vanishing contribution for large JT), we can substitute the sum over the Matsubara modes by integrals,

$$\begin{aligned} \log g^{\text{t.t.i.}}(T) &= -I_{\text{ramp}} = \frac{JT}{2\pi} \left[\int_0^2 \left(\log N \sqrt{4 - x^2} + \sum_{k \neq 0} \log \frac{1}{(1 - \lambda_k) \sqrt{1 + \lambda_k(1 - x^2 + \lambda_k)}} \right) dx \right. \\ &\quad \left. + \int_2^\infty \sum_k \log \frac{4}{(2 + \lambda_k(2 - x^2 + x \sqrt{x^2 - 4}))^2} dx \right] \\ &= \frac{JT}{\pi} \left[\log(64N/e^3) + \sum_{k \neq 0} (1 + \lambda_k) \frac{\text{arctanh} \sqrt{\lambda_k}}{\sqrt{\lambda_k}} - 1 \right]. \end{aligned} \quad (\text{S36})$$

The name I_{ramp} is due to the fact that this term is the one responsible for the exponential growing of the ramp, as it can be seen from the fact that $I_{\text{ramp}} \propto JT$.

Notice that for $\alpha \sim 0$, which implies $\lambda_k \sim 0$ for $k \neq 0$, the sum gives a negligible $O(1)$ contribution and we are left with just the first term. This result is the same as the one in Ref. [63, eq. (S29)], up to the corrections of some terms due to the fact that the vacuum volume and the one-loop contributions in that reference were not properly included.

E. Soft modes contribution

In section D we have calculated the zero-mode volume and the one-loop determinant of the time-translation-invariant fluctuations. However, as shown in Eq. (10), there are also contributions to the one-loop determinant that are not time-translation invariant. These are given by

$$\det \tilde{K}_k^{ab}(\omega_1, \omega_2)^{-\frac{1}{2}} \quad \omega_1 \neq \omega_2, \quad (\text{S37})$$

where

$$\tilde{K}_k^{ab}(\omega_1, \omega_2) = (-)^{a+b} - \frac{\lambda_k}{J^2} \tilde{\Sigma}^{aa}(\omega_1) \tilde{\Sigma}^{bb}(-\omega_2) \quad (\text{S38})$$

is the renormalized kernel, where we have already accounted for the correct path integral normalization discussed in section A. We can massage the expression for the determinant of \tilde{K} as following

$$-\frac{1}{2} \log \det \tilde{K} = -\frac{1}{2} \log \text{Tr} \tilde{K} = -\frac{1}{2} \sum_{a,b,k} \sum_{\omega_1 \neq \omega_2} \log \left((-)^{a+b} - \frac{\lambda_k}{J^2} \tilde{\Sigma}^{aa}(\omega_1) \tilde{\Sigma}^{bb}(-\omega_2) \right). \quad (\text{S39})$$

Further, we restrict the analysis to the soft modes, which are responsible for the leading contribution. The soft modes can be thought of as small deviations from the zero modes discussed around Eq. (12), so they are determined by $a \neq b$ and $|\omega_{1,2}| < 2J$, but now the two frequencies differ by a small quantity $\omega_2 = \omega_1 + \epsilon$ with $|\epsilon| = 2\pi|j|/T \ll 2J$. This last condition is met at late times, when $JT \gg 1$. Expanding \tilde{K} in the small ϵ limit, we get

$$-I_{\text{soft}} = -\frac{1}{2} \sum_{-2J < \omega_1 < 2J} \sum_k \sum_{j \neq 0} \log \left(1 + \lambda_k \left(-1 - i \frac{\text{sign}(j)\epsilon}{\sqrt{4J^2 - \omega_1^2}} \right) \right) = - \sum_{0 < \omega_1 < 2J} \sum_k \sum_{j=1}^M \log \left((1 - \lambda_k)^2 + \frac{\epsilon^2 \lambda_k^2}{4J^2 - \omega_1^2} \right). \quad (\text{S40})$$

Here, M is a positive integer counting the number of soft modes, so it must satisfy the relation $M \ll JT$.

The presence of M results in an ambiguous expression, as there is no natural choice for its value. This ambiguity can be resolved by using the analytical properties of the kernel \tilde{K} and its behaviour at infinity, which are the same as in the $\alpha = 0$ case. Following [63], the first step is to notice that

$$\int d\omega_1 d\omega_2 \log \tilde{K}_k^{ab}(\omega_1, \omega_2) = 0. \quad (\text{S41})$$

The idea now is to add this integral to regulate the determinant of the kernel and restrict it to the soft-mode contribution, which becomes

$$-I_{\text{soft}} = - \sum_{0 < \omega_1 < 2J, k} \left(\sum_{j=1}^M - \int_0^{M+\frac{1}{2}} dj \right) \log \left((1 - \lambda_k)^2 + \frac{\epsilon^2 \lambda_k^2}{4J^2 - \omega_1^2} \right). \quad (\text{S42})$$

The limits of integration have been chosen in such a way to eliminate the M dependence. In order to see this, we have to separate in the sum $\lambda_0 = 1$ from the rest of the eigenvalues, i.e., $I_{\text{soft}} = I_{\text{soft}, k=0} + I_{\text{soft}, k \neq 0}$. For $k = 0$, we have

$$-I_{\text{soft}, k=0} = - \sum_{0 < \omega_1 < 2J} 2 \left(\sum_{j=1}^M - \int_0^{M+\frac{1}{2}} dj \right) \log \left(\frac{2j\pi/T}{\sqrt{4J^2 - \omega_1^2}} \right) \sim - \sum_{\omega_1 > 0} \log \left(T \sqrt{4J^2 - \omega_1^2} \right), \quad (\text{S43})$$

where we have used Stirling's approximation for large M . Performing the sum over $\omega_1 = \pi(2n+1)/T \sim 2\pi n/T$, we get

$$-I_{\text{soft}, k=0} = -\frac{1}{2} \sum_{n < JT/\pi} \log \left[(2\pi)^2 \left(\frac{J^2 T^2}{\pi^2} - n^2 \right) \right] = \frac{JT}{\pi} \log \left(\frac{e}{4JT} \right) \quad (\text{S44})$$

where we have used again Stirling's approximation. We can evaluate in a similar way the $k \neq 0$ sum:

$$-I_{\text{soft},k \neq 0} = - \sum_{0 < \omega_1 < 2J} \sum_{k \neq 0} \left(\sum_{j=1}^M - \int_0^{M+\frac{1}{2}} dj \right) \log \left((1 - \lambda_k)^2 + \frac{(2\pi k \lambda_k / T)^2}{4J^2 - \omega_1^2} \right) \sim \frac{1}{2} \sum_{0 < \omega_1 < 2J} \sum_{k \neq 0} \log(1 - \lambda_k)^2, \quad (\text{S45})$$

and the sum over ω_1 trivially leads to

$$-I_{\text{soft},k \neq 0} = \frac{JT}{\pi} \sum_{k \neq 0} \log(1 - \lambda_k). \quad (\text{S46})$$

Summing up these two contributions, we have the 1-loop determinant (S39) can be approximated by the soft modes contribution given by

$$-I_{\text{soft}} = -I_{\text{soft},k=0} - I_{\text{soft},k \neq 0} = \frac{JT}{\pi} \log \left(\frac{e}{4JT} \right) + \frac{JT}{\pi} \sum_{k \neq 0} \log(1 - \lambda_k), \quad (\text{S47})$$

which provides the leading correction to the exponential ramp calculated in section D.

F. Analytic expression for the SFF

In this section we will explain how to derive Eq. (15). Our calculation of the SFF $g(T)$ can be thought as divided in two contributions: one determined by the classical action I_{cl} , which is relevant at early times, while the second one by the 1-loop determinant. In the previous sections, we split this last contribution into two pieces, depending on whether they contained the zero modes (section D) or not (section E). Overall, the SFF is given by

$$g(T) = e^{-I_{\text{cl}}} e^{-I_{\text{ramp}}} e^{-I_{\text{soft}}} \quad (\text{S48})$$

where the last two contributions are the one computed in the previous sections, while for evaluating I_{cl} we need to consider the action on the saddle point solution. Since the saddle point solution (7) is a site-independent, the classical action reduces to

$$-I[\tilde{\Sigma}] = \frac{1}{2} \sum_i \text{Tr} \log(\partial - i\tilde{\Sigma}) - \sum_{abj} \frac{(-)^{a+b}}{4J^2} \iint_0^T A_{ij}^{-1} \tilde{\Sigma}^{ab} \tilde{\Sigma}^{ab} = \frac{N}{2} \left[\text{Tr} \log(\partial - i\tilde{\Sigma}) - \sum_{ab} \frac{(-)^{a+b}}{2J^2} \iint_0^T \tilde{\Sigma}^{ab} \tilde{\Sigma}^{ab} \right], \quad (\text{S49})$$

which is the same action as in the $\alpha = 0$ case. This means that we can borrow the classical action contribution from the one calculated in Ref. [63], which reads

$$I_{\text{cl}} = N \log 2 + N \sum_k \frac{(-1)^k}{k} \frac{2J_1(2JkT)}{2JkT}, \quad (\text{S50})$$

where J_1 is a Bessel function of the first kind. Combining all three terms, we arrive at Eq. (15).

G. Perturbative calculation

This section aims to extend the one-loop calculation presented in section D by setting up a perturbative calculation to determine the regimes in which the saddle point solution in Eq. (7) can be trusted. In the $\alpha = 0$ case, we anticipate a well-defined perturbative series in $1/N$ as for the quadratic SYK model, however we need an understanding also of the $\alpha > 0$ case. In this section, we will use the conventions discussed in section D and we will restrict our analysis to the time-symmetric contribution to the SFF.

To evaluate perturbations around the saddle point solution $\tilde{\sigma}_n$, we need to expand the action $I[\sigma_n] = I[\tilde{\sigma}_n + \delta\sigma_n] = I[\tilde{\sigma}_n] + \delta I_n[\delta\sigma_n]$ to higher orders with respect to the quadratic one considered in Eq. (S29). Differently from what we have done in section D, we will expand the fluctuations on the Fourier basis:

$$\delta I_n[\delta\sigma_n] = -\frac{1}{2} \sum_i \sum_{m \geq 2} \frac{(-1)^m}{m} \text{Tr} \left[\left(\tilde{\sigma}_n \sum_k \frac{e^{\frac{2\pi i}{N} jk}}{\sqrt{N}} \delta\sigma_n^k \right)^m \right] - \sum_k \frac{1}{\lambda_k} \text{Tr}(\delta\sigma_n^k \delta\sigma_n^{-k}), \quad (\text{S51})$$

where now $\delta\sigma_n^{-k} = (\delta\sigma_n^k)^\dagger$. We now separate the quadratic part of δI_n , which we name $\delta I_n^{(2)}$, from the higher orders, and then expand the exponential of the higher-order terms in a power series. At each order of this expansion, the integral is Gaussian and can therefore be performed explicitly, provided that we can determine the propagator, which is needed for evaluating the Wick contractions.

The quadratic action reads

$$\delta I^{(2)}[\delta\sigma_n] = -\frac{1}{2} \sum_{k,l \geq 0} \sum_{abcd} (\delta\sigma_n^{-k})_{ab} (\delta\sigma_n^l)_{cd} K_{ab,cd}^{k,l}. \quad (\text{S52})$$

Here we defined the inverse propagator

$$K_{ab,cd}^{k,l} = \delta_{ac} \delta_{bd} \delta_{kl} ((\tilde{\sigma}_n)_{aa} (\tilde{\sigma}_n)_{bb} + \lambda_k^{-1}), \quad (\text{S53})$$

which is nothing but Eq. (10) in the new conventions and restricting to the time-translation invariant case. Notice that for $x_n < 2$ we have spontaneously broken symmetries, which requires to remove the zero modes that correspond to $k = 0$ before inverting K . Taken care of this subtlety, K is diagonal in the indices (k, a, b) , and it can be easily inverted to give the propagator:

$$(K^{-1})_{ab,cd}^{k,l} = \delta_{ac} \delta_{bd} \delta_{kl} \frac{\lambda_k}{(\tilde{\sigma}_n)_{aa} (\tilde{\sigma}_n)_{bb} \lambda_k + 1}. \quad (\text{S54})$$

Excluding the classical action and 1-loop contribution, which do not play a role in the discussion, a generic perturbative expansion is defined by

$$\langle e^{\delta I_n - \delta I_n^{(2)}} \rangle = \sum_{\alpha} \frac{1}{\alpha!} \langle (\delta I_n - \delta I_n^{(2)})^{\alpha} \rangle \quad (\text{S55})$$

where now $\langle \bullet \rangle$ indicates the normalized Gaussian integration with measure $\delta I_n^{(2)}$. The non-quadratic terms $\delta I_n - \delta I_n^{(2)}$ can be seen as interaction vertices and are given by

$$\delta I_n - \delta I_n^{(2)} = -\frac{1}{2} \sum_i \sum_{m \geq 3} \frac{(-1)^m}{m} \text{Tr} \left[\left(\tilde{\sigma}_n \sum_k \frac{e^{\frac{2\pi i}{N} jk}}{\sqrt{N}} \delta\sigma_n^k \right)^m \right]. \quad (\text{S56})$$

Since an odd number of $\delta\sigma_n$ insertion would result in a vanishing contribution, the first non-trivial term C in the perturbative expansion is given by setting $\alpha = 1$ and $m = 4$. More explicitly this term reads:

$$\begin{aligned} C &= -\frac{1}{8} \sum_j \sum_{k_1 \dots k_4} \sum_{a_1 \dots a_4} \frac{e^{\frac{2\pi i}{N} j(k_1 + \dots + k_4)}}{N^2} (\tilde{\sigma}_n)_{a_1 a_1} \dots (\tilde{\sigma}_n)_{a_4 a_4} ((\delta\sigma_n)_{a_1 a_2}^{k_1} (\delta\sigma_n)_{a_2 a_3}^{k_2} (\delta\sigma_n)_{a_3 a_4}^{k_3} (\delta\sigma_n)_{a_4 a_1}^{k_4}) \\ &= -\frac{3}{8} \sum_{k_1, k_2} \frac{1}{N} \left[\sum_a \frac{\lambda_{k_1} (\tilde{\sigma}_n)_{aa}^2}{(\tilde{\sigma}_n)_{aa}^2 \lambda_{k_1} + 1} \cdot \frac{\lambda_{k_2} (\tilde{\sigma}_n)_{aa}^2}{(\tilde{\sigma}_n)_{aa}^2 \lambda_{k_2} + 1} \right], \end{aligned} \quad (\text{S57})$$

Due to the presence of the eigenvalues λ_k , this expression is hard to evaluate explicitly, but we can extract the large- N behaviour in the relevant cases. Let's start by considering the case where $\alpha = 0$. The only eigenvalue which does not scale with $1/N$ is $\lambda_0 = 1$, while we have $\lambda_{k \neq 0} = 1/N$. Since $\tilde{\sigma}$ is order $O(1)$, we have

$$C = O(1/N), \quad \alpha = 0. \quad (\text{S58})$$

We expect this to still be true for $\alpha \gtrsim 0$, since just a small number of eigenvalues with small k are $O(1)$, as discussed in section C. However, for $\alpha > 1/2$ most of the eigenvalues become $O(1)$, giving the following contribution to the first term in the perturbative expansion

$$C = O(N), \quad \alpha > 1/2. \quad (\text{S59})$$

We expect the transition $C = O(1)$ to happen around $\alpha = 1/2$, in correspondence to the kink of λ_k , even if a more in-depth study would be needed to confirm this. This signals the breakdown of the saddle-point approximation for $\alpha > 1/2$, which can be due either to entering a non-perturbative regime or to the appearance of a new saddle point.

Notice that, in principle, we could have considered terms with $m > 4$ in Eq. (S56). For $\alpha = 0$ this would have led to subleading contributions respect to $m = 4$ due to the higher factors of $1/\sqrt{N}$ coming from the Fourier coefficient in equation (S56). For $\alpha > 1/2$ we don't need to consider more contributions because if just one term becomes non-perturbative, the whole series is.

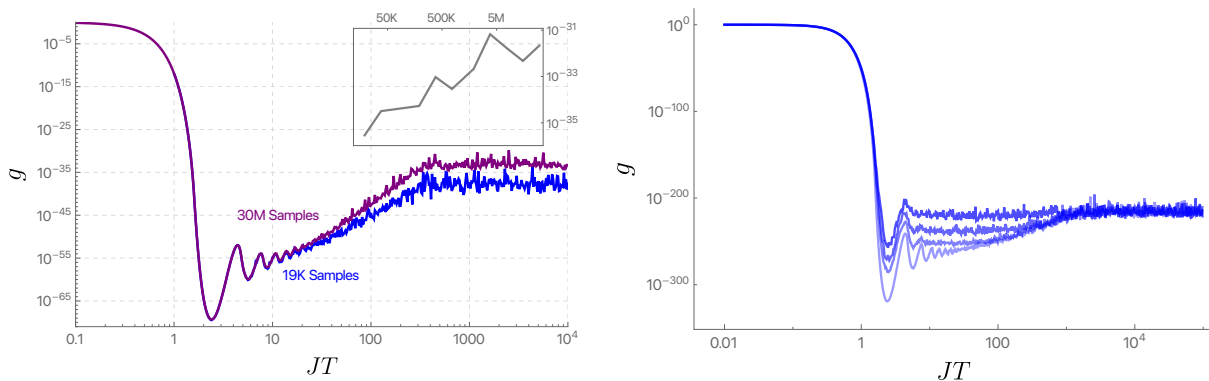


FIG. S1: Left panel: The SFF for $N = 200$ and $\alpha = 0$, averaged over 19K samples (blue) and 30M samples (violet). The two curves are offset relative to each other, with the gap increasing over time and saturating at the plateau. The theoretical plateau value is $2^{-N/2} = 8 \cdot 10^{-31}$. The inset shows the averaged plateau value (computed over both time and samples) as a function of the number of samples. Right Panel: The SFF for $N = 900$ and 50K samples at $\alpha = 0, 0.9, 1.1, 1.5$ (from lighter to darker shades of blue). Compared to the $N = 200$ case shown in Figure 1b, the secondary plateau is significantly longer and flatter.

H. Details on the numerics

For the numerical analysis, the SFF has been reduced to the single particle eigenvalues μ_i of the hopping matrix $a_{ij}J_{ij}$ similarly to what has been done e.g. in [64] for complex fermions:

$$g(T) = \prod_{\mu_i > 0} \cos^2 \left(\frac{\mu_i T}{2} \right). \quad (\text{S60})$$

While this expression allows to accelerate considerably the numerical simulation and explore quite large system sizes compared to $\text{SYK}_{q>2}$ models, the quadratic SYK exhibits extremely large fluctuations in the ramp regime even for $\alpha = 0$. These fluctuations scale as $(N/T)^T$ [76], presenting a challenge for accurately averaging the SFF in systems with large N .

Insufficient statistical averaging leads to noticeable artifacts in the SFF, as illustrated in Fig. S1. These include not only large fluctuations but also a systematic downward shift of the SFF. This effect is particularly prominent in the late-time plateau, which stabilizes below the theoretical value of $2^{-N/2}$. This shift is also at the origin of the displacements between the various curves in 3, which however can be corrected by a constant shift, as shown in the inset.

This limitation restricts us to relatively small sizes compared to those achievable with exact diagonalization of the hopping matrix, leaving to the secondary plateau less time to develop. An example of the SFF for $N = 900$ is shown in Fig. S1. Although the statistical sample size is insufficient, as evidenced by the compression of the SFF after the slope, it is still apparent that the secondary plateau is significantly longer and flatter compared to that in Fig. 1.